Origin of Friction Anisotropy on a Quasicrystal Surface

Aleksander E. Filippov,[1] Andrea Vanossi,[2,3] and Michael Urbakh[4]

[1]*Donetsk Institute for Physics and Engineering of NASU, 83144, Donetsk, Ukraine*
[2]*International School for Advanced Studies (SISSA) and CNR-IOM Democritos National Simulation Center, Via Beirut 2-4, 34014 Trieste, Italy*
[3]*CNR-INFM National Research Center S3 and Department of Physics, University of Modena and Reggio Emilia, Via Campi 213/A, 41100 Modena, Italy*
[4]*School of Chemistry, Tel Aviv University, 69978 Tel Aviv, Israel*

(Received 17 September 2009; published 19 February 2010)

Wearless friction force experiments [Science **309**, 1354 (2005)] have recently demonstrated that tribological response in quasicrystals could be related to the exotic atomic structure of the bulk material. Here, by numerical simulations, we address the origin of the experimentally observed friction anisotropy on a twofold decagonal quasicrystal surface. We predict the distinct stick-slip patterns in the lateral force along the periodic and quasiperiodic directions, specifically exploring the temperature dependence that rules the transitions between single and multiple-slip regimes of motion.

DOI: 10.1103/PhysRevLett.104.074302 PACS numbers: 46.55.+d, 07.79.Sp, 61.44.Br, 68.37.Ps

Advances in several research fields have led to a progressive change of paradigm during the last decades, as the concept of order without periodicity has emerged to properly describe an increasing number of complex systems. Shortly after the discovery of quasicrystals [1], it was realized that their well-ordered, yet nonperiodic structure is dictated by a rule other than periodicity and closely related to the description of incommensurate structures, as in the nonperiodic mathematical constructions giving rise to the 1D Fibonacci sequence or the 2D Penrose tiling [2]. Early experimental measurements showed that the intriguing quasicrystal structure goes hand-in-hand with physical properties (e.g., hardness) that are unusual, in light of their chemical composition [3]. Because of their long-range atomic order but no spatial translational invariance, they have lately attracted much attention as a class of increasingly interesting tribological materials, showing anomalously low coefficients of friction and high scratch resistance. To unravel the most intriguing hypothesis that their frictional response could be related to the exotic atomic structure of the bulk material, friction force microscopy (FFM) experiments have been recently done [4–6] in the regime of ''wearless'' friction. A significant anisotropy in friction has been observed by dragging the FFM tip along the periodic and aperiodic directions of a twofold decagonal Al-Ni-Co quasicrystal surface. While most known quasicrystals are icosahedral, with quasiperiodic bulk structure in all three dimensions, the decagonal quasicrystals have a structure presenting both periodic and aperiodic atomic arrangements in the same surface [7], allowing *in situ* experimental comparisons of friction along crystalline and quasicrystalline directions.

In this Letter we investigate through numerical simulations the fundamental aspects of quasicrystal wearless friction related to their intrinsic peculiar morphology. By implementing an on-site substrate potential, closely mimicking the structural features of the twofold decagonal Al-Ni-Co surface, and in the framework of a Tomlinson model, we are able to reproduce the experimentally observed anisotropic tribological response. We predict the distinct stick-slip patterns in the lateral force occurring for the periodic and quasiperiodic directions, specifically exploring the temperature dependence that governs the transitions between single and multiple-slip regimes of motion.

Two-dimensional frictional motion of the FFM tip pulled along a quasicrystalline surface can be modeled by the following coupled Langevin equations [8]:

$$m\partial^2 x/\partial t^2 + \gamma \partial x/\partial t + K(x - V_x t) + \partial U(x, y)/\partial x = f_x,$$
$$m\partial^2 y/\partial t^2 + \gamma \partial y/\partial t + K(y - V_y t) + \partial U(x, y)/\partial y = f_y, \quad (1)$$

where m is the tip effective mass, and x and y are its surface coordinates. The tip is pulled by a spring of effective constant K connected to a microscope support that moves with a constant velocity $\mathbf{V} = \{V_x, V_y\}$. Then the instantaneous lateral friction force, measured in FFM experiments, reads as $\mathbf{F} = -K\{x - V_x t, y - V_y t\}$. We assume the same damping coefficient γ, accounting for the dissipation to the degrees of freedom not explicitly included in the model, in both x and y directions. The effect of thermal fluctuations is given by the δ-correlated random forces $f_x(t)$ and $f_y(t)$, $\langle f_{x,y}(t) f_{x,y}(t')\rangle = 2\gamma k_B T \delta(t - t')$. The values of the model parameter m and K were chosen to fit the experimental conditions, and for γ we used typical values from previous FFM simulations [9–12].

The two-dimensional tip-surface potential, $U(x, y)$, has been generated by an *ad hoc* numerical procedure, in order to mimic the interaction of the tip with the twofold decagonal quasicrystal surface [13]. Figure 1 shows a collage of an atomically resolved STM image of a fragment of the

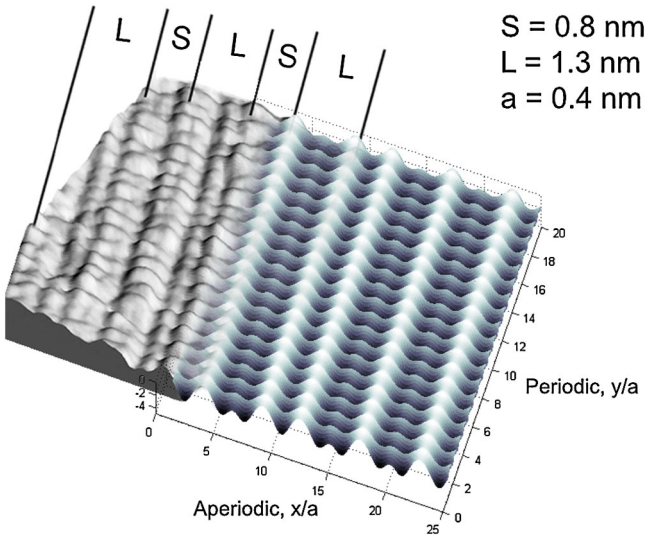

FIG. 1 (color online). Collage of the STM image of a fragment of twofold Al-Ni-Co surface [6] with the numerically generated potential (3). Al atomic rows along the periodic y axis exhibit periodicity of $a = 0.4$ nm. In the aperiodic x direction, these rows are separated by short and long distances ($S = 0.8$ nm, $L = 1.3$ nm) following the Fibonacci sequence. The surface topography is well reproduced by a surface potential (3) composed of a set of anisotropic Gaussian functions.

Al-Ni-Co twofold surface [6] and the numerically generated potential, $U(x, y)$. The STM surface topography reveals the presence of atomic rows along the periodic tenfold direction, y, with spatial periodicity $a = 0.4$ nm. Along the orthogonal axis in the surface plane (the aperiodic x direction), two different characteristic lengths $S = 0.8$ nm and $L = 1.3$ nm, as highlighted in the figure, separate the rows and define the sizes of pseudo unit cells. The L and S distances form a Fibonacci sequence [7], with a ratio L/S close to the golden mean $\tau = (1 + \sqrt{5})/2 = 1.618\ldots$. In order to reproduce geometrical features of the Al-Ni-Co surface topography, we approximated the tip-surface potential $U(x, y)$ by a sum of anisotropic Gaussians $G_{kk'}(x, y) = U_0 \exp[-(x - X_k)^2/w_1 - (y - Y_{k'})^2/w_2]$, spatially centered at the equivalent positions of the Al atoms. These positions $(X_k, Y_{k'})$ form a 2D array in the x-aperiodic and y-periodic directions [14]:

$$X_k = S\left[\tau\left\|\frac{k}{\tau}\right\| + \left(k - \left\|\frac{k}{\tau}\right\|\right)\right], \quad Y_{k'} = ak', \quad k, k' = 1, 2, \ldots, \tag{2}$$

where the symbol $\|\|$ denotes the closest integer number to the argument. To fit the experimentally observed surface structure [6], we introduced an anisotropy of local potentials by setting the two different widths, $w_1 = 0.4$ nm and $w_2 = 1.0$ nm, along the x and y directions, respectively, in the Gaussians. Then the resulting twofold quasicrystal potential can be written in as

$$U(x, y) = U_0 \sum_{k,k'} G_{kk'}(x, y). \tag{3}$$

In order to understand an origin of the observed friction anisotropy [4], we performed calculations of tip trajectories and friction forces for different directions of the tip pulling along the surface. The direction of pulling is defined by the angle, ϑ, between the pulling velocity V and the x axis; thus, $\vartheta = 0$ and $\vartheta = \pi/2$ correspond to the outermost x-aperiodic and y-periodic directions, respectively. For a given pulling direction we evaluated the x and y components of the mean friction force, $F_x = \langle \overline{K(V_x t - x)}^t \rangle$ and $F_y = \langle \overline{K(V_y t - y)}^t \rangle$, by averaging the instantaneous forces over sufficiently long time runs and large ensemble of realizations. The results presented in Fig. 2(a) clearly demonstrate the angular anisotropy of the friction force that has been calculated for the quasicrystal surface of Fig. 1. Our calculations show that in accordance with experimental observations [4–6] the frictional force in the aperiodic direction (dots) is significantly lower than that in the periodic direction (open circles). It should be noted that pulling the *point* tip [as described by Eqs. (1)] precisely along the periodic y direction gives a very low friction force, $\langle F \rangle = 0.4$ nN, that reflects a presence of grooves with a weak potential corrugation in this direction (see Fig. 1). However, due to the tip finite size and "imperfectness" of the pulling, such low friction cannot be observed experimentally, and we do not show this value in Fig. 2(a). Already 1° deviation from the perfect y direction results in a much higher force, $\langle F \rangle = 40$ nN, as presented in Fig. 2(a).

What is the origin of the angular anisotropy of friction found in our simulations? For the Al-Ni-Co quasicrystal surface the characteristic length scales of potential corrugation along the aperiodic direction ($S = 0.8$ nm and

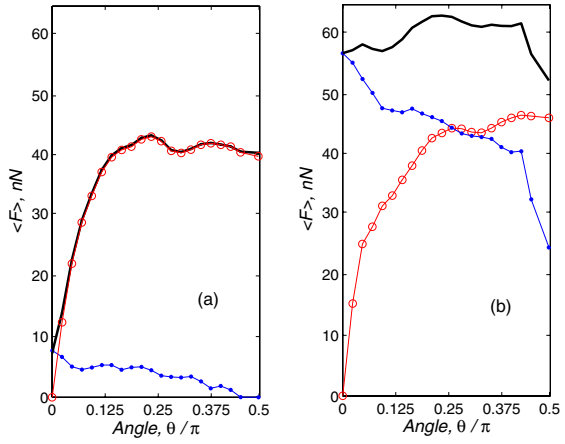

FIG. 2 (color online). Dependence of the mean friction force (bold curves) and its projections on the periodic (open circles) and aperiodic (dots) axes on the pulling direction. (a) Numerical results for the twofold Al-Ni-Co surface shown in Fig. 1; (b) numerical results for a model quasicrystal surface which exhibits identical corrugation lengths along the periodic and aperiodic directions; i.e., $S \equiv a = 0.4$ nm and $L = \tau S$. Other parameters: $\gamma = 5 \times 10^{-6}$ kg/s, $U_0 = 4 \times 10^{-20}$ J, $m = 5 \times 10^{-11}$ kg, $V = 150$ nm/s, $K = 1.5$ N/m, $T = 40$ °K.

$L = 1.3$ nm) are substantially larger than the potential period along the periodic direction ($a = 0.4$ nm). As a result for the same amplitudes of potential corrugation the force experienced by the tip in the x direction is considerably lower than that in the y direction. To be certain that this is the main reason for the friction anisotropy, we calculated $\langle F \rangle$ for a "model" quasicrystal potential which exhibits essentially identical corrugation lengths along both periodic and aperiodic axes; i.e., the small distance S equals the period in the y direction, $a = 0.4$ nm, and the long segment, $L = \tau S$ [see Fig. 2(b)]. Keeping all other parameters the same as in Fig. 2(a), we found [see Fig. 2(b)] that the friction force along the aperiodic axis (dots) increases drastically and becomes comparable with the force in the periodic direction (open circles). This analysis demonstrates that the difference between the length scales of potential corrugation in the periodic and aperidioc directions is the main source of the observed anisotropy of friction on the Al-Ni-Co quasicrystal surface.

The difference between potential profiles in the aperiodic and periodic directions manifests itself in a time series of friction forces and tip displacement as shown in Fig. 3. Here the friction response has been simulated by pulling the support at the angle $\vartheta = \pi/4$ and calculating the x and y projections of the tip displacement and force. Similar results have been obtained for different directions of pulling. In both aperiodic and periodic directions we observed multiple-slip regimes of motion, where the tip slips over a number of "lattice" spacing [15,16]. The tip trajectories in the aperiodic direction exhibit slips with lengths close to S and L, while in the periodic direction we observe slips over one, two, and three periods of the potential. The corresponding segments of tip motion are highlighted by the horizontal dashed lines in Figs. 3(b) and 3(d). It should be noted that because of the creep motion of the tip in the stick phase, the jump lengths during the slip events are considerably shorter than the corresponding distances between the substrate potential minima. The contribution of the creep to the overall motion is more pronounced for the pulling along the aperiodic direction where the stiffness of the surface potential is lower than that for the periodic direction.

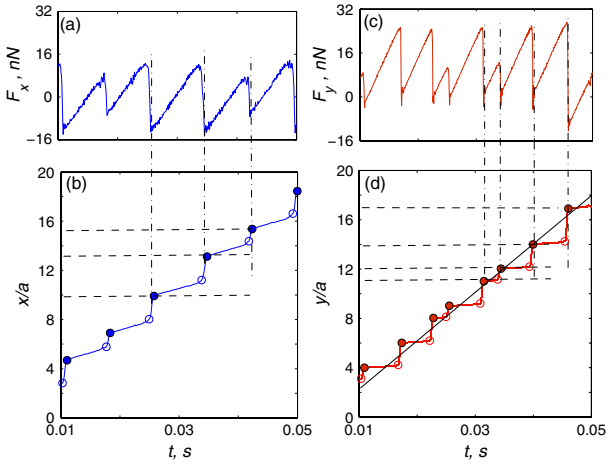

FIG. 3 (color online). Time series of friction forces and corresponding tip trajectories, obtained for the pulling at the angle $\vartheta = \pi/4$. Panels (a),(b) and (c),(d) show the friction response in the x-aperiodic and y-periodic directions, respectively. Dashed lines in (b) and (d) mark two characteristic length scales, $S = 2a$ and $L = 2\tau a$, observed for the stick-slip motion in the aperiodic direction and three lengths, a, $2a$, $3a$ for the periodic directions. All parameters are as in Fig. 2.

It has been found recently that the slip lengths change with temperature, and this effect may strongly influence a temperature dependence of friction [17]. In order to get insight into mechanisms of temperature dependence of friction on quasicrystals, we show in Fig. 4 the probability distribution functions (PDFs) for the slip lengths, $P(L)$, which have been calculated from the time series of the tip displacement along the aperiodic and periodic directions for two temperatures, $T = 40$ K and $T = 400$ K. Figure 4 shows that at low temperature, $T = 40$ K, the tip pulled along the aperiodic direction performs mainly slips corresponding to S and L spacings, while for the periodic direction we observe single, double, and triple slips. We note again that because of the creep motion of the tip the PDF maxima for the aperiodic direction are located at considerably lower lengths than the characteristic ones, S and L. This, of course, may present difficulties in interpretation of experimental data and in identification of surface topographies from FFM measurements.

Figure 4 demonstrates a strong effect of temperature on the PDFs for the slip lengths, showing that for both periodic and aperiodic directions the mean slip length decreases with increase of temperature. However, the microscopic origins of this effect are different for these two directions. Figure 4(a) shows that at high temperature, $T = 400$ K, a new, short-length peak appears in the PDF for the aperiodic direction that is missing at low tempera-

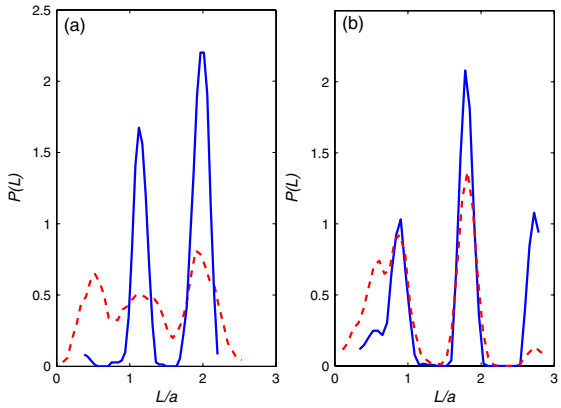

FIG. 4 (color online). Probability distribution functions (PDFs) for slip lengths in aperiodic (a) and periodic (b) directions for the same parameters as in Fig. 3. Solid and dashed curves correspond to low and high temperatures, $T = 40$ and 400 K, respectively. Maxima in the PDFs correspond to the characteristic lengths marked in Fig. 3. The parameters are as in Fig. 2.

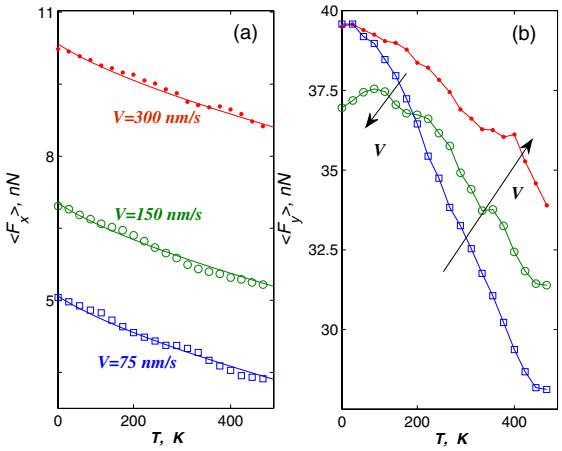

FIG. 5 (color online). Temperature dependencies of the mean friction force in the aperiodic (a) and periodic (b) directions for three pulling velocities: $V = 75$ nm/s (squares), 150 nm/s (circles), and 300 nm/s (dots). Solid lines in (a) show analytical estimations according to the equation, $\langle F \rangle = F_c - BT^{2/3}\ln^{2/3}(BT/V)$. In the panel (b) temperature intervals exhibiting distinct velocity dependencies of the friction force are marked by the oppositely oriented arrows, which show a direction of velocity increase. The parameters are as in Fig. 2.

tures. This peak corresponds to thermally activated jumps of the tip back and forth between the accessible wells of the potential during a stick-slip event [18,19]. As a result for high temperatures the peaks in $P(L)$ corresponding to S and L spacings are suppressed compared to those for low temperatures. For the periodic direction the increase of temperature leads to a significant reduction of the probability of the triple slips and to a slight reduction of the double slip contribution.

Finally, in Fig. 5 we present temperature dependencies of the mean friction force in the aperiodic (left panel) and periodic (right panel) directions calculated for three different pulling velocities $V = 75$ nm/s(squares), 150 nm/s(circles) and 300 nm/s (dots). For the aperiodic direction the mean friction force decreases monotonically with temperature following the law, $\langle F \rangle = F_c - BT^{2/3}\ln^{2/3}(BT/V)$, where F_c is the value of the friction force at $T = 0$. This behavior may be explained by thermally activated jumps of the tip over the potential barrier which cause a reduction of friction [9–12]. The emergence of back and forth jumps of the tip, that is the main effect of T on the slip length PDF for the aperiodic direction, only slightly influences the mean friction force. Figure 5(b) shows that the friction in the periodic direction exhibits a richer temperature dependence with a peak or/and plateau at cryogenic temperatures. This nontrivial temperature dependence of $\langle F \rangle$ is caused by a suppression of triple slips and a considerable reduction of the mean slip length with increase of T, which lead to an increase of the energy dissipation per unit length. Figure 5(b) also demonstrates that the friction forces, $\langle F(V) \rangle$, calculated for different temperatures show contrasting V behaviors: increase, decrease, or no change with V. These effects have been discussed in details recently [17].

To summarize, we have proposed a model that describes the strong angular anisotropy of friction recently observed at the Al-Ni-Co quasicrystal surface [4–6], and anticipates an interesting friction temperature dependence ruling the transitions between single and multiple-slip regimes. The friction anisotropy arises due to a difference in substrate corrugation length scales in the aperiodic and periodic directions. An additional contribution, not accounted for here, may also come from a difference in phonon dissipation along the aperiodic and periodic axes, where the dispersion bands might show energy gaps due to the Fibonacci sequence of distances and masses. Finally, we point out the potential that certain aperiodic mathematical constructions (e.g., the Fibonacci sequence and Penrose tiling), have to describe phenomena appearing in different fields, such as biophysics, pattern formation in space/time, electronic and optical technological applications.

We thank Ron Lifshits and Erio Tosatti for useful discussion. This work, as part of the ESF EUROCORES Program FANAS (ACOF, AFRI, AQUALUBE), was supported by Israel Science Foundation (1109/09) and Italian CNR. A. V. and A. F. thank the School of Chemistry at Tel Aviv University for the kind hospitality. M. U. thanks the financial support by Italian CNR Short-term Mobility.

[1] D. Shechtman *et al.*, Phys. Rev. Lett. **53**, 1951 (1984).
[2] See, e.g., R. Penrose, *Aperiodicity and Order*, edited by M. V. Jaric (Academic, Boston, 1989), Vol 2, p. 53.
[3] See, e.g., Z. M. Stadnik, *Physical Properties of Quasicrystals* (Springer-Verlag, Berlin, 1999).
[4] J. Y. Park *et al.*, Science **309**, 1354 (2005).
[5] J. Y. Park *et al.*, Phys. Rev. B **72**, 220201(R) (2005).
[6] J. Y. Park *et al.*, Phys. Rev. B **74**, 024203 (2006).
[7] W. Steurer, Z. Kristallogr. **219**, 391 (2004).
[8] A. Vanossi and O. M. Braun J. Phys. Condens. Matter **19**, 305017 (2007).
[9] Y. Sang, M. Dube, and M. Grant, Phys. Rev. Lett. **87**, 174301 (2001).
[10] O. Dudko *et al.*, Chem. Phys. Lett. **352**, 499 (2002).
[11] P. Steiner *et al.*, Phys. Rev. B **79**, 045414 (2009).
[12] I. Szlufarska, M. Chandross, and R. W. Carpick, J. Phys. D **41**, 123001 (2008).
[13] J. B. Suck, M. Schreiber, and P. Häussler, *Quasicrystals: An Introduction to Structure, Physical Properties, and Applications* (Springer, Berlin, 2004).
[14] R. Lifshitz, J. Alloys Compd. **342**, 186 (2002).
[15] K. L. Johnson and J. Woodhouse, Tribol. Lett. **5**, 155 (1998).
[16] S. N. Medyanik *et al.*, Phys. Rev. Lett. **97**, 136106 (2006).
[17] Z. Tshiprut, S. Zelner, and M. Urbakh, Phys. Rev. Lett. **102**, 136102 (2009).
[18] D. Abel, S. Yu. Krylov and J. W. M. Frenken, Phys. Rev. Lett. **99**, 166102 (2007).
[19] Z. Tshiprut, A. E. Filippov and M. Urbakh, J. Phys. Condens. Matter **20**, 354002 (2008).